X-524-71-343

HEAVY ION PLASMA CONFINEMENT IN AN RF QUADRUPOLE TRAP

J-P. Schermann

F. G. Major

July 1971

Goddard Space Flight Center
Greenbelt, Maryland

CONTENTS

	Page
INTRODUCTION	1
PRODUCTION AND RECOMBINATION OF ION PAIRS	2
1. Production of Ion Pairs by Photoabsorption	2
2. Experimental Data	4
3. Ion-Ion Recombination	6
MOTION OF IONS IN AN RF QUADRUPOLE TRAP	8
1. Single Particle Motion	8
2. Frequencies of Motion of Plasma Ions Trapped in a Quadrupole Field	12
3. Survival Equations in RF Quadrupole Trap	17
APPARATUS	19
1. Vacuum System	19
2. Ion Quadrupole Trap	19
3. Ultraviolet Lamps	21
4. Ion Detector	23
EXPERIMENTAL PROCEDURE AND RESULTS	27
FUTURE WORK	31
REFERENCES	32

HEAVY ION PLASMA CONFINEMENT IN AN RF QUADRUPOLE TRAP

INTRODUCTION

An atomic frequency standard uses as a reference the hyperfine resonance of an atomic system localized in an environment as free as possible from perturbations. The electrodynamic suspension of ions in high vacuum permits a higher degree of isolation than conventional means of confinement of neutral particles (buffer gases, non-disorienting walls) and an incomparably longer time of observation than atomic beams. The basic limitation, so far, for any practical application (laboratory primary standard, spaceborne clock) is the number of ions which can be contained. The ions will necessarily generate a space-charge repulsive field which counteracts the trapping fields of the confining device. The simultaneous confinement of positive and negative ions, leading to space-charge neutralization, in a quadrupole RF electrostatic cage, has been proposed by F. G. Major [1], as a means to increase the number of trapped ions. The confinement of plasmas with electrons has been extensively studied, mostly for thermonuclear-fusion experiments. On the other hand, the properties of heavy ion plasmas have only recently been investigated.[2] [3]

This paper considers the confinement of an electron-free plasma in a pure quadrupole RF electric trap. The ultimate goal of this work was to produce a large density of mercury ions, in order to realize a trapped ion frequency standard using the hyperfine resonance of 199 Hg^+ at 40.7 GHz. At first an attempt was made to obtain an iodine plasma consisting of equal numbers of positive and negative ions of atomic iodine, the positive iodine ions being susceptible to charge-exchange with mercury atoms will produce the desired mercury ions. The experiment showed that the photoproduction of ions pairs in iodine using the necessary uv radiation occurs with a small cross-section, making it difficult to demonstrate the feasibility of space charge neutralization in a quadrupole trap. For this reason it was considered expedient to choose thallium iodide, which has a more favorable absorption spectrum (in the region of 2000-2100 Å). The results indicate that, although the ionic recombination is a serious limiting factor, a considerable improvement can be obtained in practice for the density of trapped ions, with a considerable advantage in lifetimes for spectroscopic purposes. The ion pair formation by photoionization is briefly reviewed. A continuous spectrum lamp and a nearly monochromatic lamp are compared by means of an ionization chamber. A simple theory is derived for relating the ion densities to the frequencies of motion of the ions in a quadrupole field. The experimental values for the densities deduced with the aid of this calculation are then compared with lifetime measurements, with reasonable agreement.

PRODUCTION AND RECOMBINATION OF ION PAIRS

1. Production of Ion Pairs by Photoabsorption

Ions can be produced by electron or photon bombardment of molecules. Different typical processes are shown in Table I.

Electron Bombardment	Photon Bombardment
$AB + e \rightarrow A^- + B$ Dissociative Resonant Capture	$AB + h\nu \rightarrow AB^+ + e$
$AB + e \rightarrow A^+ + B^- + e$ Ion Pair Formation	$AB + h\nu \rightarrow A^+ + B^-$
$AB + e \rightarrow AB^-$ Resonant Attachment	$AB + h\nu \rightarrow A^+ + B + e$

Of these processes, we will consider only ion-pair formation by means of photon bombardment. The other processes involve electrons which would have a negative space charge field complicating or preventing the conditions of space charge neutrality.

A typical potential energy diagram of a molecule in which the ion-pair formation process occurs, is shown in figure 1, where only the energy levels relevant to this process are represented.

The ground state may be represented by a Morse potential

$$U(r - r_0) = D_0 \left[1 - \exp\left(-\beta (r - r_0)\right)\right]^2$$

where D_0 is the dissociation energy and r_0 the equilibrium internuclear distance of the ground state molecule.

For internuclear distances large enough to neglect the exchange forces, the potential energy for the state involved in pair formation, is simply the 1/r coulomb attraction energy between the ions. The upper level potential energy corresponds to the polarization attraction between a charged particle and an induced dipole. The different reactions of photoionization involve the absorption of a photon in an allowed transition of the molecule from the ground state to some upper electronic state. The Frank-Condon[4] principle states that the

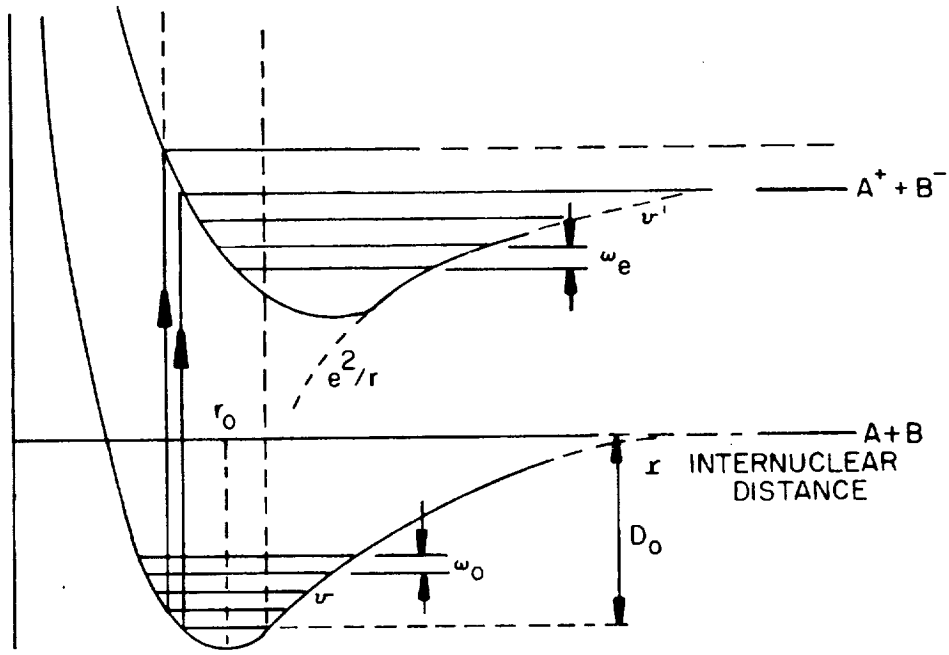

Figure 1. Molecular energy states and transitions between vibrational states which will lead to dissociation into ion pairs.

largest transition probabilities correspond to transitions occurring vertically in the potential energy diagram.

The cross sections are proportional to the square of the overlap integral of the vibrational wave functions of the neutral ground state and the excited state (Frank-Condon factors):

$$\sigma \sim \left| \int \psi_v(R)\, \psi_{v'}(R)\, dR \right|^2 = \left| F(v, v') \right|^2$$

If ω_0 represents the vibrational frequency in the ground state, the distribution of populations between the different vibration levels is a Boltzmann distribution $\exp[-m\omega_0/kT]$ when m is an integer. For example, the experimental cross section in the region of threshold of the process $TlI + h\nu \rightarrow Tl^+ + I^-$ (figure 6) may be fitted with a curve derived from the various contributions of the vibrational levels.[5]

The threshold energy corresponding to ion-pair formation can be computed if one knows:

- the molecular ground state dissociation energy D_0
- the ionization potential of the electropositive atom $A + E_0 \rightarrow A^+ + e$
- the electron affinity of the electronegative atom $B + e^- \rightarrow B^- + E_A$

The critical photon energy $h\nu$ is then equal to

$$h\nu = D_0 + E_0 - E_A.$$

These quantities are shown in table II for the molecules I_2 and TlI.

Table II

Molecule	I_2	TlI
r_0 (Å)	2.7	2.9
D_0 (ev)	1.54	2.64
E_0 (ev)	10.45	6.1
E_A (ev)	3.06	3.06
$h\nu$ (ev)	8.93 (1390 Å)	5.68 (2180 Å)

2. Experimental Data

The Halogens

The photoproduction of ion pairs in the halogens is a process with a rather large cross section,[6] thus for the reaction $I_2 + h\nu \rightarrow I^+ + I^-$ the cross-section peaks at 40×10^{-18} cm^2 for a wavelength of $\lambda = 1380$ Å. This may be compared with the reaction $I_2 + h\nu \rightarrow I_2^+ + e$ which has a cross-section of 75×10^{-18} cm^2 (at 1215 Å Lyman α). Figure 2 shows the dependence of these cross-sections on photon energy.

Thallium Halides

The thallium halides can produce ion pairs by photoabsorption.

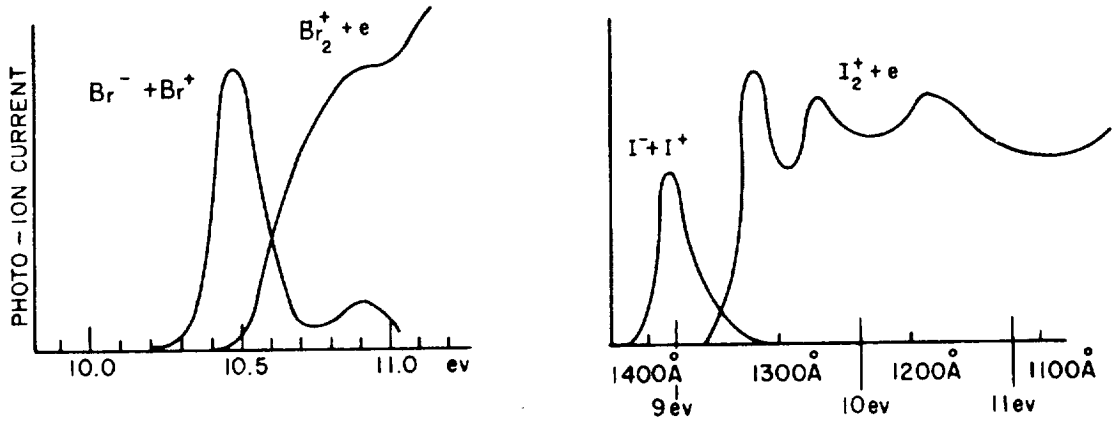

Figure 2. Photoionization and pair production in the halogen molecules Br_2, I_2.

The cross sections, shown in their dependence on photon energy in Figures 3a and 3b are smaller than for molecular iodine. Berkowitz[5] gives the following values

$$TlI + h\nu\ (1335\text{Å}) \rightarrow Tl^+ + I \qquad \sigma \approx 5 \times 10^{-18}\ cm^2$$

$$TlI + h\nu\ (2100\text{Å}) \rightarrow Tl^+ + I^- \qquad \sigma \approx 1 \times 10^{-18}\ cm^2$$

The imprecision for the second value is quite large. Terenin[ ] gives $\sigma = 3 \times 10^{-18}\ cm^2$.

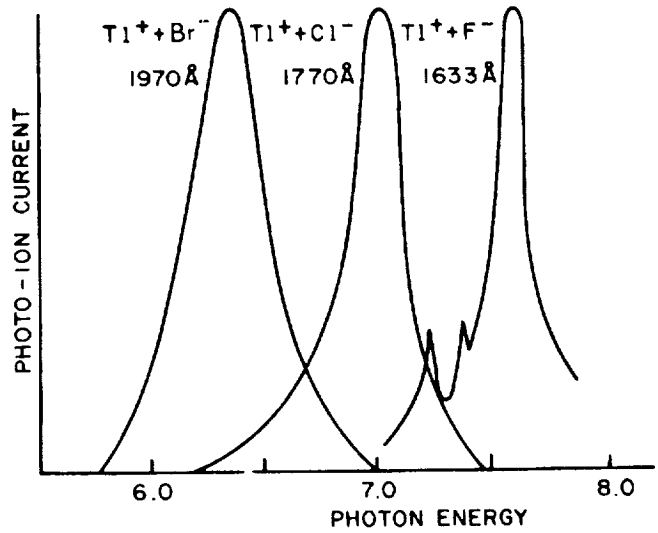

Figure 3a. Photoproduction of ion pairs in the halides of thallium TlBr, TlCl, and TlF.

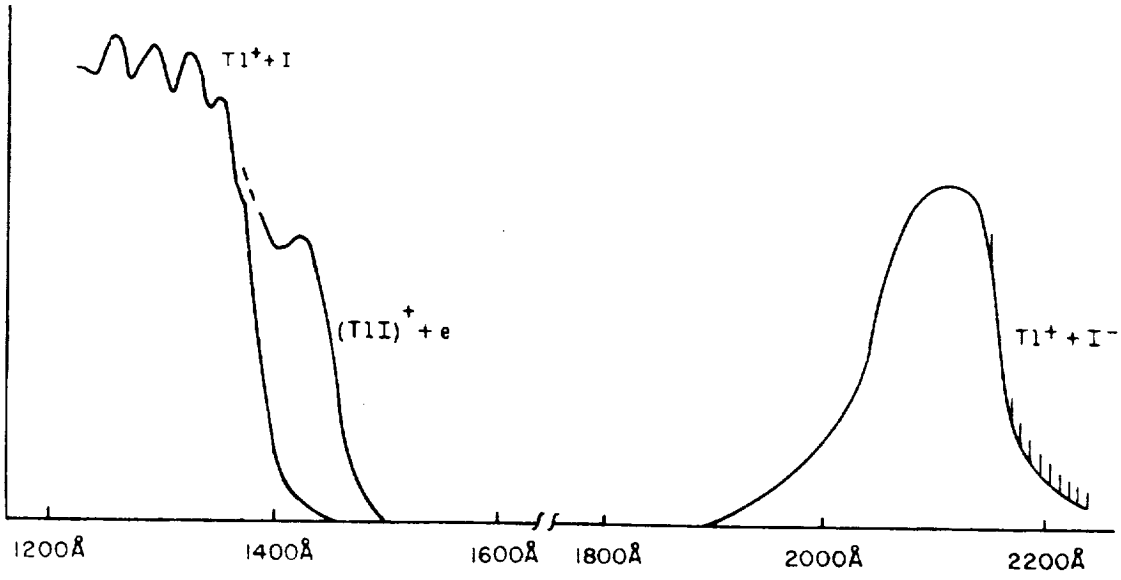

Figure 3b. Photoproduction of ion pairs and photoionization of the T l molecule.

3. Ion-Ion Recombination

The recombination process is a very important limiting factor for the production of a heavy ion plasma. For very low pressures, recombination occurs by means of the process of charge exchange.

$$A^+ + B^- \rightarrow A^* + B^* \rightarrow (A + B + \text{fluorescence})$$

If R is the number of recombination events per unit volume and unit time, n^+ and n^-, the respective densities of positive and negative ions, the recombination coefficient α is defined by:

$$R = \alpha n^+ n^-$$

For thallium iodide, the molecular potential energy levels relevant to recombination are shown in figure 4.

In a collision between a positive and negative ion, the potential energy curves of the ionic system interset with the atomic system curves at some rather large internuclear distance, where there is a finite probability for the system to jump from the ionic state to the atomic state. The probability can be computed

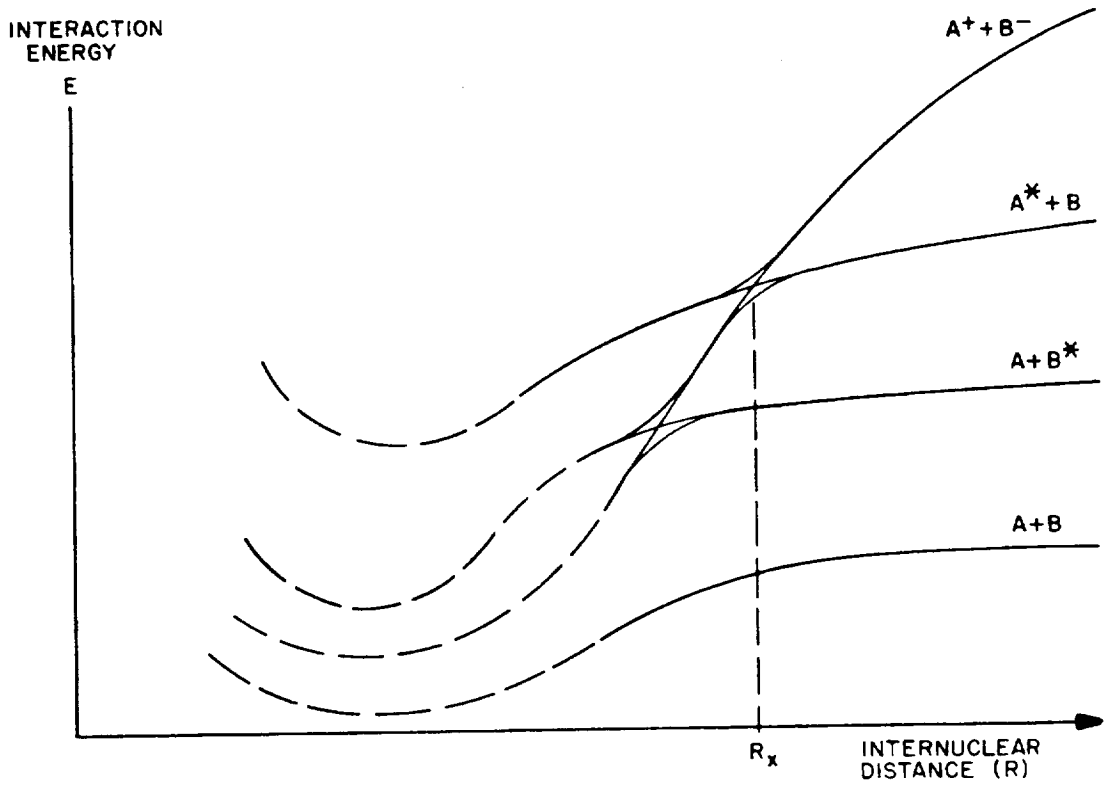

Figure 4. Psuedo-crossings of molecular energy status leading to transition to molecular status that are assymptotically not ionic.

from the Landau-Zener theory.[8] If the criterion for recombination is that the centers of mass of the ions reach a separation equal to or less than the largest crossing value R_x, the recombination coefficient, for a Maxwellian distribution, is given, to a first approximation by

$$\alpha = \pi R_x^2 \, [8 \, k \, T/\mu \pi]^{1/2} \, [1 + e^2/R_x \, k \, T]$$

where kT is the energy of the ions and μ the reduced mass. For the $Tl^+ - I^-$ system, the recombination coefficient is plotted as a function of the energy of the ions in figure 5. The corresponding cross sections are extremely large (10^{-13} -10^{-12} cm^2) and this process can easily be predominant.

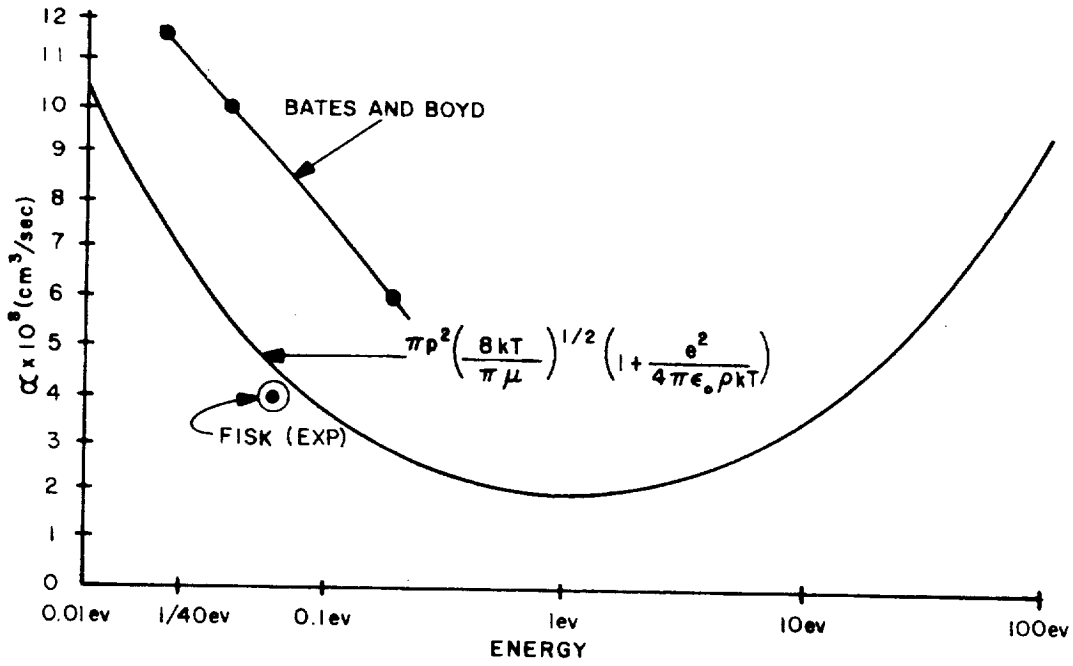

Figure 5. Recombination coefficient α, computed as a function of impact energy.

MOTION OF IONS IN AN RF QUADRUPOLE TRAP

A purely electric quadrupole field can be generated by a set of electrodes as shown in figure (6a) with $r_0 = \sqrt{2} z_0$. The potential applied to the electrodes is the sum of a static potential V_{DC} and a sinusoidal potential with amplitude V_{AC} and frequency Ω.

1. Single Particle Motion

The equations of motion in the r and z directions for a single ion with mass m and charge e, can be transformed to have the form of the Mathieu equation

$$a^2 x_i / d\tau^2 + (a_i + 2 q_i \cos 2\tau) x_i = 0$$

where

$$\tau = \Omega t / 2, \quad a_r = -\frac{1}{2} a_z = \frac{4 e V_{DC}}{m r_0^2 \Omega^2}, \quad q_r = \frac{1}{2} q_z = \frac{2 e V_{AC}}{m r_0^2 \Omega^2}$$

The solutions of these equations can be stable or unstable depending on the coefficients a_i and q_i. Thus an ion may be confined in the trap only for values

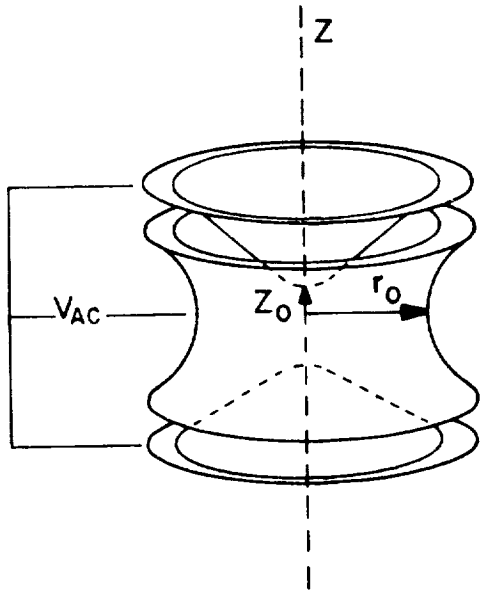

Figure 6a. Electrode geometry of the quadrupole rf ion trap.

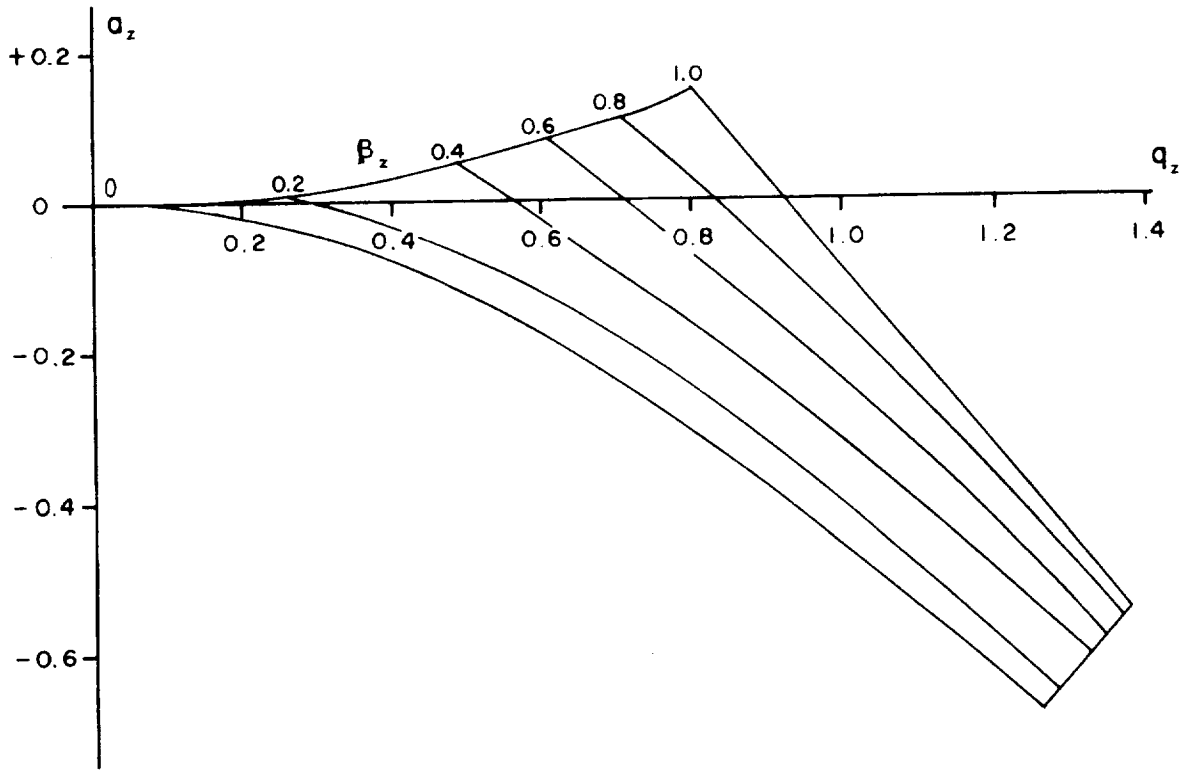

Figure 6b. Stability diagram for one particle motion in an rf quadrupole field.

of V_{DC}, V_{AC}, and Ω such that the corresponding values of a and q are in a stable region of the (a,q) plane. The first stable region is shown in figure (6b). For small values of a and q, it may be shown that the Mathieu equations have solutions of the form:

$$x_i(\tau) = A\left[1 + \frac{1}{2} q_i \cos 2\tau\right] \cos \beta_i \tau$$

where

$$\beta_i = [a_i + q_i^2/2]^{1/2}$$

The ion motion in the trap is then a harmonic oscillation, for each coordinate r and z, at a frequency

$$\omega_i = \frac{\beta_i \Omega}{2},$$

on which is superimposed a micromotion at frequency Ω.

One can show that the average motion is governed by a scalar potential field given by

$$e\phi = \frac{1}{8} m \Omega^2 (\beta_r^2 r^2 + \beta_z^2 z^2)$$

It is convenient to specify the maximum depth of the potential field ϕ_m, which gives the limit on the trapped ion energy.

The following values of the parameters have been used in the experiments described below:

axial dimension of the trap	$z_0 = 1.0$ cm
radial dimension	$r_0 = 1.42$ cm
effective volume of the trap	$V = 6$ cm^3
trapping frequency	$\Omega/2\pi = 230$ kHz
axial oscillation frequency	$\omega_z/2\pi = 23$ kHz
axial potential well depth	ϕ_m { = 2.2 volts (Tl^+) = 1.37 volts (I^-)

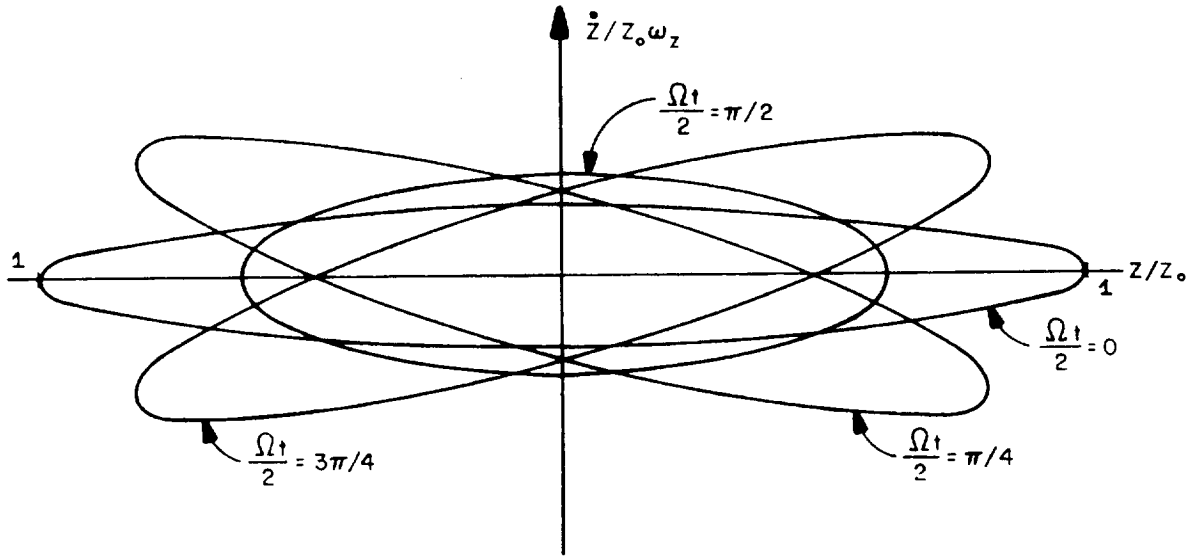

Figure 7a. Boundaries in the $\dot{z}/\omega_z z_0$, z/z_0 plane for the initial velocity and position of an ion in order to be confined within the trap plotted for different initial of phase.

An ion will be confined within the trap if it was created at a time t_0 with values of position $x_i(t_0)$ and velocity $\dot{x}_i(t_0)$ such that the maximum displacement x_{im} does not exceed the dimensions of the trap. It has been shown by Paul [10] that,

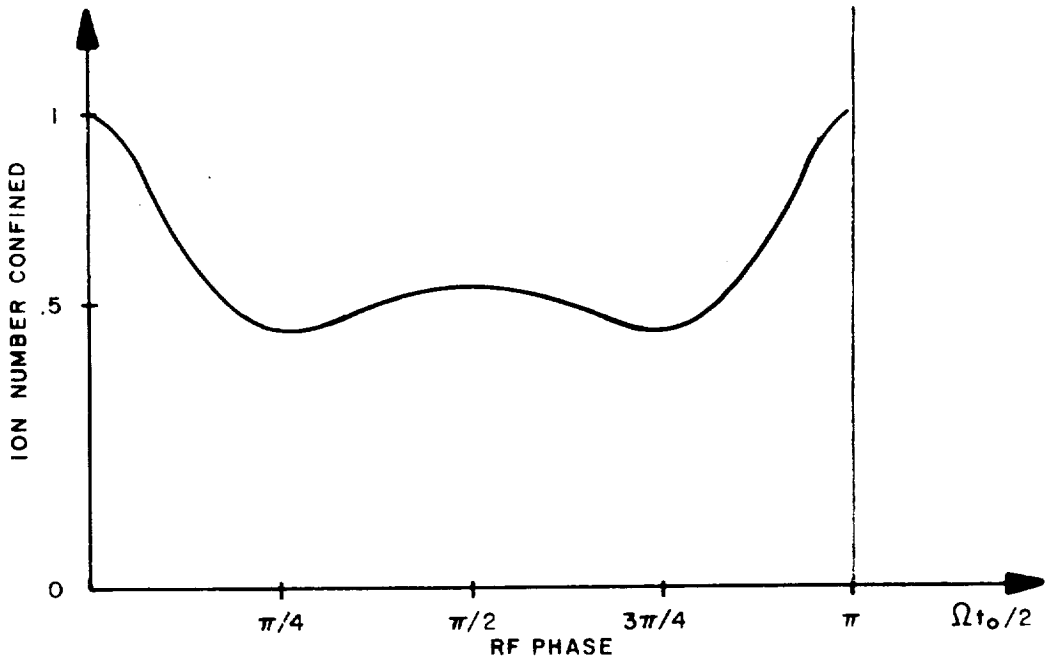

Figure 7b. Fraction of ions uniformly produced in the volume of the trap which will be confined, plotted as function of the initial rf phase.

for a given t_0, the value of $(x_i/x_{im}, \dot{x}_i/\omega_i x_{im})$ must lie inside an ellipse shown in figure (7a). For the value of $\beta_z = 0.2$ the fraction of ions starting from rest which have a given maximum amplitude is plotted versus the initial phase $\omega t_0/2$ of the trapping field in figure (7b). If the initial phases of the RF field for the different ions is assumed to be randomly distributed, only 66% of the created ions will be trapped.

In order to confine positive and negative ions with respective masses m^+ and m^-, the operating points in the (a,q) diagram must be restricted to the intersection of the two stability diagrams of the ions with a scale factor $-[m^+/m^-]$. This is shown in figure 8 for thallium and iodine.

2. Frequencies of Motion of Plasma Ions Trapped in a Quadrupole Field

It has been so far assumed that the ions constitute a very dilute gas, without mutual interactions. As the density rises, the space charge field developed by the ions (if a single sign of charges is present) tends to overcome the binding energy provided by the quadrupole field. In the trap of radius 1.4 cm, the binding energy of 2ev is exceeded when the density is greater than 3×10^7 ions cm^{-3}. Previous experimental work[11] indicates a practically attainable value for the

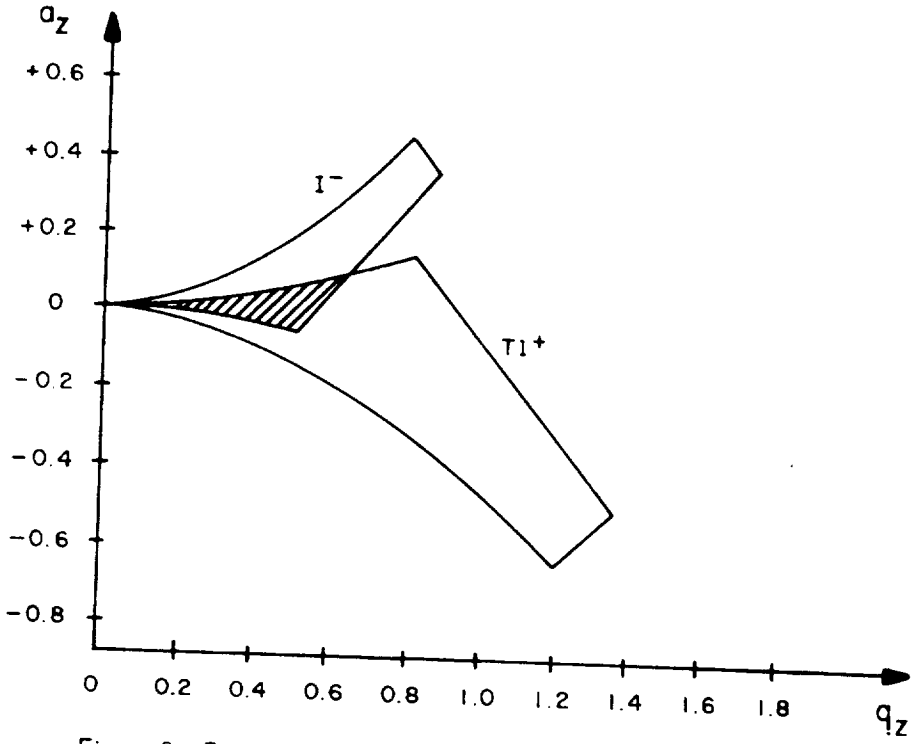

Figure 8. Composite plot of stability regions for Tl^+ and I^- ions in a quadrupole rf trap.

density even lower than predicted by the space-charge limit. Less than 2×10^5 ions cm^{-3} have been reported in a potential well of 6eV.

When ions of both signs are confined, each of the ions is surrounded by an ion cloud whose net charge is equal and opposite to that of the ion itself. The measure of the size of the screening ion cloud is given by the Debye length $\lambda_D = (\epsilon_0 \, kT/ne^2)^{1/2}$ where n is the charge density, see figure 9. The interaction potential between particles has a shorter range than the Coulomb potential,

$$\phi_{ij} = \frac{1}{4\pi\epsilon_0} \frac{e_i \, e_j}{r} \exp\left[-r/\lambda_D\right]$$

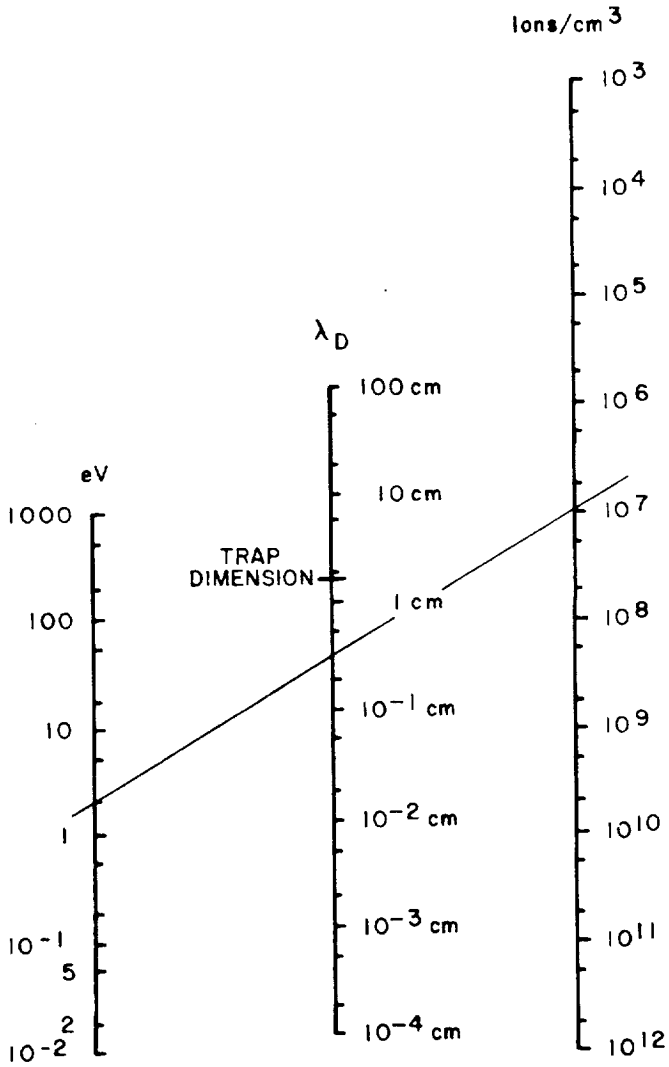

Figure 9. Nomogram relating the Debye length λ_D to the temperature and ion density.

For a density of 2×10^7 ions cm^{-3} and a binding energy of 2eV, the Debye length is 3mm, a distance smaller than the trap dimensions. The ions can be considered as forming a plasma. At this density, the mean distance between ions is 4×10^{-3} cm corresponding to approximately 10^6 ions in a sphere with radius equal to λ_D. Only waves with high enough frequency can propagate in the plasma. If the frequency is too low, the charges have time to rearrange themselves to screen the interior of the plasma from the oscillation field. It can be shown that a plasma subjected to a small perturbation will oscillate with a characteristic frequency $\omega_p = (ne^2/\mu)^{1/2}$, where n is the ion density and μ the reduced mass. Figure 10 gives a plot of ω_p as a function of ion density.

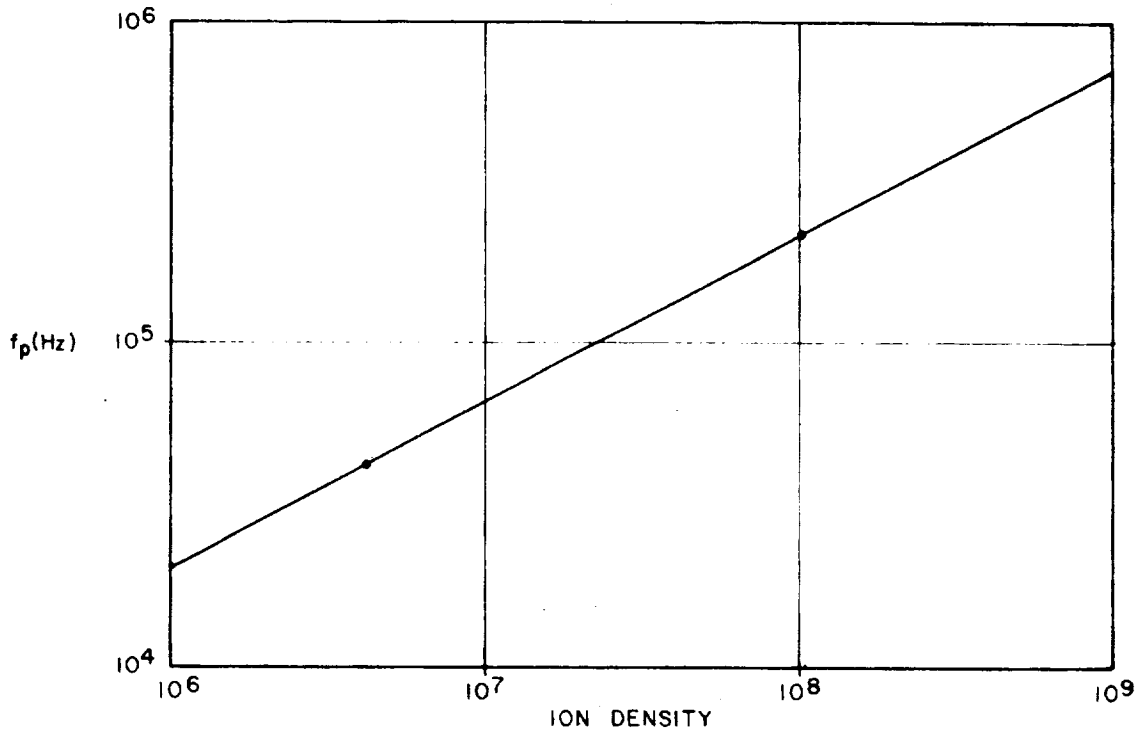

Figure 10. Plasma frequency $f_p = 1/2\pi \sqrt{ne^2/\mu}$ plotted against ion density n.

In the limit of very low densities, the different ions in the quadrupole trap have independent harmonic motions in the potential well. The equation of motion of a particle with mass m and spring constant k, along the z-direction is

$$m\ddot{z} + k\,z = 0$$

Consider two types of particles, positive ions with parameters m^+ and k^+, and negative ions with m^- and k^-. Between the j^{th} charged particle and the n^{th} there

is a force F_{nj}. The equations of motion of the different particles are now coupled

$$m^+ \ddot{z}_n + k^+ z_n = \sum_j^+ F_{nj} + \sum_j^- F_{nj} ,$$

with a similar equation for the negative ions where $\Sigma^{\pm}$ denotes summation over the positive or negative ions. Summing over all the positive charges, one obtains the equation of motion of the center of mass of positive charges, z^+

$$m^+ \ddot{z}^+ + k^+ z^+ = \sum_n^+ \sum_j^- F_{nj}$$

The forces between particles with the same sign cancelled ($F_{nj}^+ = - F_{jn}^+$). The term

$$\sum_n^+ \sum_j^- F_{nj}$$

corresponds to the force of interaction between the positive and negative ion clouds. It will be assumed that the system is in stable equilibrium and consider only small oscillations around the stable configuration. The interaction potential energy can be expanded in a Taylor series,

$$U = U_0 + \left(\frac{\partial U}{\partial z}\right)_0 \delta z + \frac{1}{2}\left(\frac{\partial^2 U}{\partial z^2}\right)_0 (\delta z)^2$$

where $\delta z = z^+ - z^-$ is the distance between the centers of charge of the ion clouds. The term $(\partial U/\partial Z)$ must vanish for equilibrium and one has

$$U = U_0 + \frac{1}{2}\left(\frac{\partial U}{\partial z}\right)_0 (z^+ - z^-)^2.$$

Hence the equations of motion become

$$m^+ \ddot{z}^+ + k^+ z^+ + C (z^+ - z^-) = 0$$

$$m^- \ddot{z}^- + k^- z^- - C (z^+ - z^-) = 0$$

where C represents the coupling between the two ion clouds due to the electrostatic interaction between the individual charged particles. With solutions of the form:

$$z^+ = a^+ e^{i\omega t}, \quad z^- = a^- e^{i\omega t},$$

the eigen-frequencies of the coupled oscillation are determined as the two positive roots ω_1, ω_2 of the secular equation,

$$\begin{vmatrix} k^+ + C - m^+ \omega^2 & - C \\ - C & k^- + C - m^- \omega^2 \end{vmatrix} = 0$$

With the following definitions

$$\omega_\pm = (k^\pm / m^\pm)^{1/2}, \quad \omega_p = (C (m^+ + m^-)/m^+ m^-)^{1/2}$$

the eigen-frequencies are given by

$$\omega_{1,2}^2 = \frac{1}{2} (\omega_+^2 + \omega_-^2 + \omega_p^2) \pm \frac{1}{2} \left\{ (\omega_+^2 + \omega_-^2 + \omega_p^2)^2 \right.$$

$$\left. - 4 \left[\omega_+^2 \omega_-^2 + \frac{\omega_p^2}{m^+ + m^-} (m^+ \omega_+^2 + m^- \omega_-^2) \right] \right\}^{1/2}$$

These solutions ω_1, ω_2 are plotted in Figure 11, for different values of the plasma frequency ω_p, as a function of the operating potentials on the trap, that is, the free uncoupled oscillation frequencies ω_+ and ω_-.

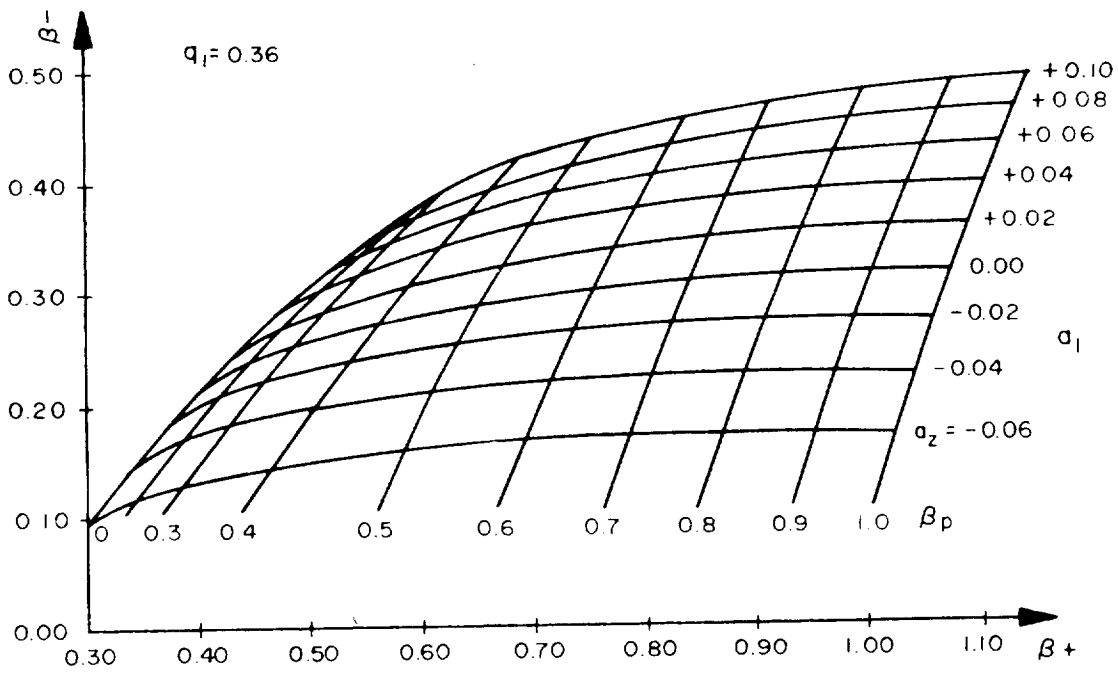

Figure 11. The eigen-frequencies of mass 204 (Tl^+) and mass 127 (I^-) ions executing coupled oscillations in a quadrupole rf trap.

3. Survival Equations in RF Quadrupole Trap

The ions in the trap inevitably experience collisions among themselves, as well as with the background molecules from which they are formed, and by design, with a light background gas added to dampen the ion motion.

As an approximate collision interval for ion-ion collisions, one can take the value from Spitzer[12]

$$\tau_{ii} = \frac{1.4\,\mu^{1/2}\,(3kT)^{3/2}}{8\pi n e^4 \ln \Lambda}$$

μ is the reduced mass of the ionic system, T the temerpature, n the ionic density, and Λ is the ratio of the cut-off distance for the Coulomb interaction of an ion to that of closest approach: $\Lambda = 12\pi n\,(kT/4\pi ne^2)^{3/2}$. For a mean energy of the ions of 2eV and an ionic density of 10^7 ion/cm^3, one finds for ionized thallium iodide $\tau_{ii} \approx$ 2 sec, a favorably long time.

Elastic collisions between the ions and the more massive background molecules from which they are formed, lead to rf heating of the ions. It can be shown[13]

that, for a well-defined mean collision time τ_c, there is a purely exponential energy increase in time $\bar{W} = \bar{W}_0 \exp(\zeta t/\tau_c)$ where $\bar{W}$ is the ion energy averaged over a period of the RF trapping field, and ζ is a number dependent on the mass ratio of the colliding particles. Thus, if the ions experience collision with a rest gas with a smaller mass, such as helium or neon, ζ is negative and the mean kinetic energy of the ions is lowered. Experimentally, this corresponds to a considerable lengthening of the lifetime of the ions in the trap, the ions being cooled and having a lower rate of "evaporation" from the potential well. If the density of positive and negative ions are respectively n^+ and n^-, and if the creation rates are Q^+ and Q^-, the rate equations can be written

$$d n^{\pm}/d t = Q^{\pm} - n^{\pm}/\tau^{\pm} - \alpha n^+ n^-$$

These two equations are coupled through the recombination process represented by the $\alpha n^+ n^-$ term. If the ionic density is high enough, an appreciable departure from neutrality will develop a space charge field which exceeds the trapping field leading to an accelerated loss of the surplus ions and a restoration of neutrality. It can thus be assumed that $n^+ = n^- = n$, and since in ion-pair formation the rates of production of positive and negative ions are equal, $Q^+ = Q^- = Q$, the rate equations reduce to

$$d n/d t = Q - \alpha n^2 - n/\tau$$

If only one species of ions is present, the mutual neutralization does not occur and the decay is exponential.

When recombination dominates however, the decay is no longer exponential but follows the law

$$n^{-1}(t) = n^{-1}(0) + \alpha t$$

Note that for any given time t, the number of ions remaining is always less than $(\alpha t)^{-1}$ independent of the initial ion number.

APPARATUS

1. Vacuum System

The quadrupole trap was in a Pyrex vacuum system provided with a quartz window for uv illumination as shown in figure 12. This vacuum chamber was evacuated by a 1-l/s ion pump giving an ultimate pressure of approximately 5×10^{-9} Torr after bake-out. The pump was connected through a stainless steel valve. The thallium iodide was distilled into a sidearm and independently temperature controlled to control the vapor pressure. The most satisfactory operation was obtained by enclosing the trap chamber in an oven while keeping the valve and the pump at room temperature. In order to avoid any deposit of TlI on the quartz window, the oven temperature was 300°C, about 100°C more than the maximum sidearm temperature. Helium could be introduced by means of a standard quartz leak.

2. Ion Quadrupole Trap

The trap electrodes were made by shaping expanded tantalum mesh with a computer-shaped stainless-steel mandrel having the proper quadrupole geometry.

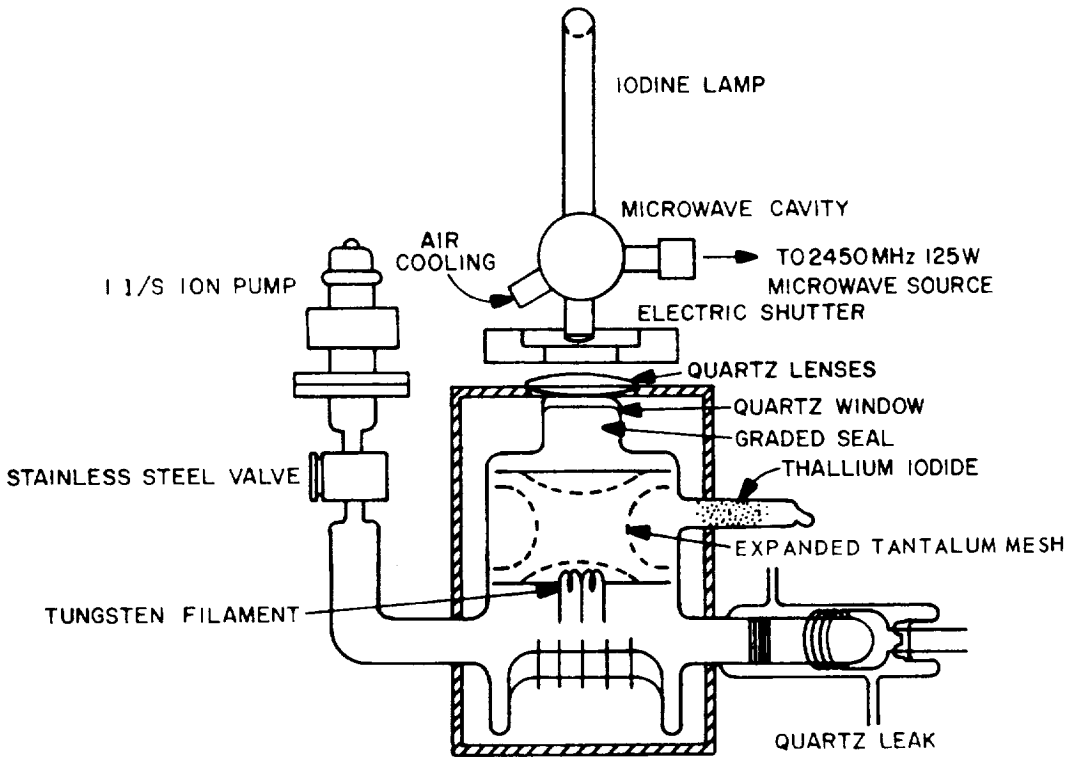

Figure 12. Apparatus for studying heavy ion plasma confinement in an rf quadrupole field.

Molybdenum rings and tantalum brackets were used to support the electrodes and connect them to the tungsten feedthrough leads.

The source of the RF trapping voltage was a 230 kHz oscillator followed by a tuned amplifier capable of providing 50 - 200 V variable amplitude at the trap. A positive or negative going sawtooth of variable amplitude and duration was obtained from a Tektronix 160 system and operational amplifiers to adjust the amplitude and the DC levels. This sawtooth could be triggered, with a variable delay, by an electrically controlled light shutter situated between the uv lamp and the trap.

The detection of the ions was accomplished by the resonant excitation of the axial motion of the center of charges [13], by a weak RF dipole field applied between the end cap electrodes from a parallel tank-circuit (Q = 100). The ion frequency of motion was varied through the fixed resonance frequency of the detection circuit (23 kHz) by linearly sweeping the DC voltage. The RF voltage appearing on the parallel tank-circuit was amplified, filtered, detected, and displayed on an oscilloscope whose horizontal deflection was driven by the ramp generator, see figure 13.

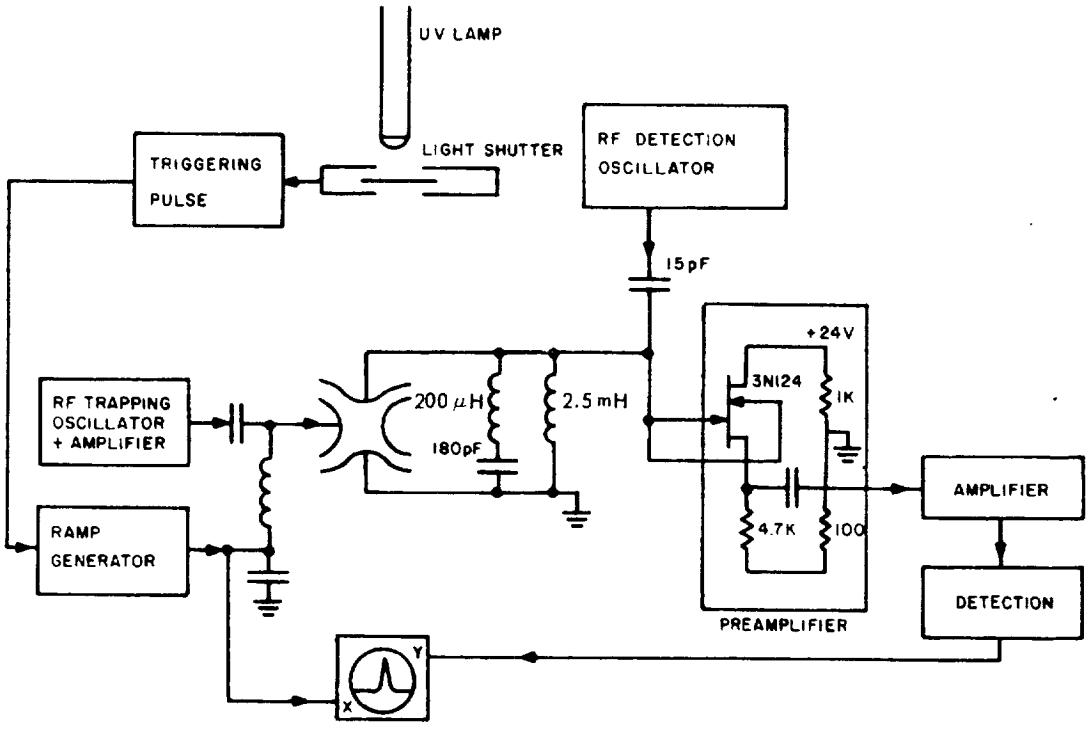

Figure 13. Block diagram of the electronics to operate the quadrupole rf trap.

3. Ultraviolet Lamps

Pair formation in iodine occurs for wave lengths shorter than 1400Å. Two processes can occur (see figure 2).

$$I_2 + h\nu\ (1410 - 1320\ A) \rightarrow I^+ + I^-$$

$$I_2 + h\nu\ (1350 \text{ and below}) \rightarrow I_2^+ + e$$

A high pressure (200 torr) krypton lamp was built with a barium fluoride window which cuts off below 1350Å (see figure 14) and hence eliminates the second process. The sealing of the barium fluoride window proved to be more difficult

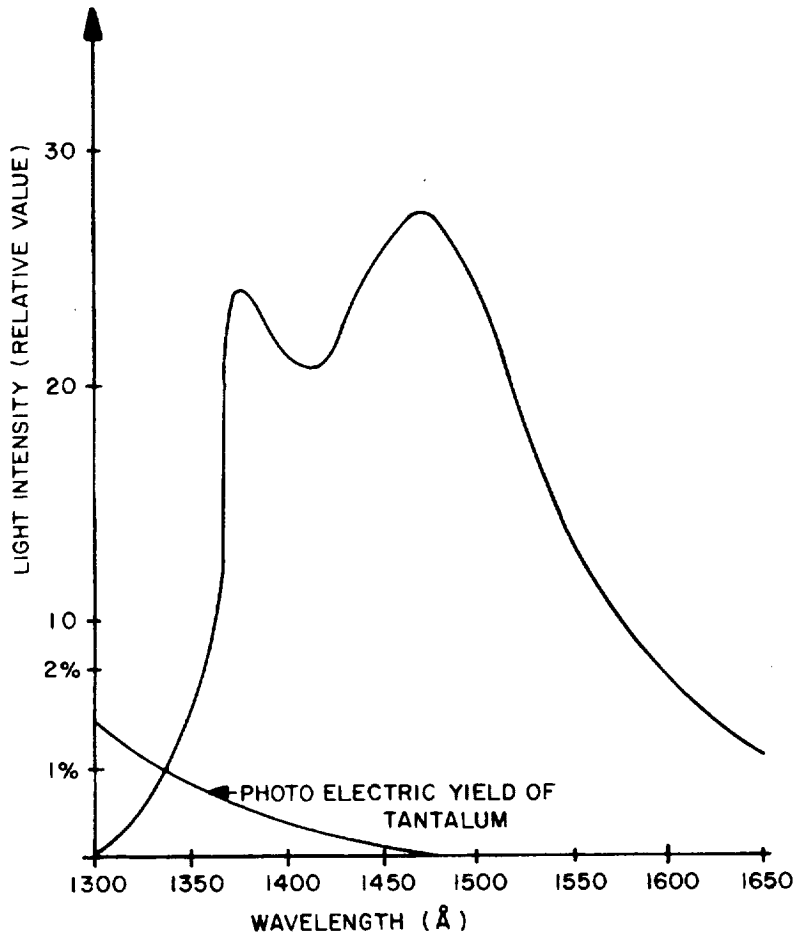

Figure 14. Spectral distribution of intensity from high pressure krypton lamp with BaF_2 window at 30°C.

than a common lithium fluoride window; thus the silver chloride method of sealing proved unsuccessful and epoxy was finally used. The lamp was filled following the procedure described by Wilkinson [14]. After bake-out under vacuum, the lamp was filled with 200 torr of krypton while flashing a titanium getter (see figure 15). The atmospheric absorption is extremely strong at 1400A and helium was continuously flushed between the lamp and the system. Two types of excitation was used: (1) a microwave cavity excited by a 125W Raytheon microwave generator at 2450 MHz, (2) a VHF oscillator at 235 MHz with inductive coupling. The high frequency discharge was found to be quite efficient and could be run from an 80 watt generator.

Pair-formation in thallium iodide on the other hand occurs between 1900Å and 2200Å, peaking around 2100Å[5]. The atomic line of iodine between the $5\ ^2P_{1/2}$ and $6\ ^2P_{3/2}$ levels [resonance radiation], is very strong and lies at 2062Å; hence an iodine lamp was built with a quartz envelope and 12 mm diameter window. After bake-out and distillation of iodine, the lamp was sealed off. No significant change in output intensity was observed after intermittent operation for a period of five months. The spectral output in the photoionization region is shown in figure 16. Approximately 4% of the total output lies in the 2062Å line. The lines at 1876Å, 1844Å, 1830Å, 1799Å are strongly absorbed by the

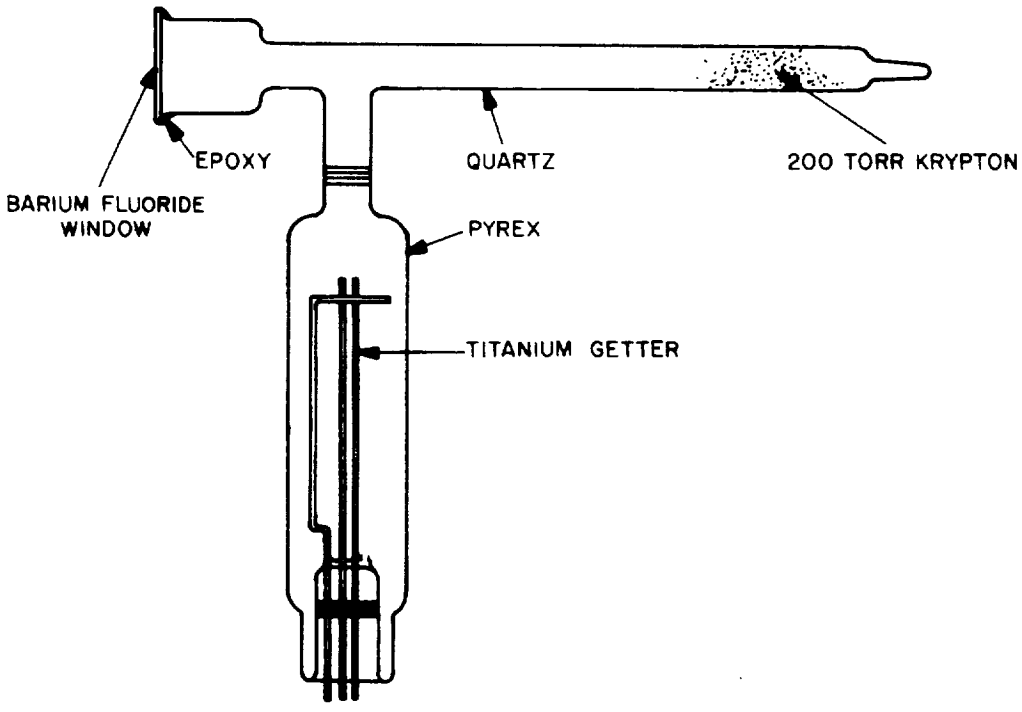

Figure 15. Design of the krypton lamp.

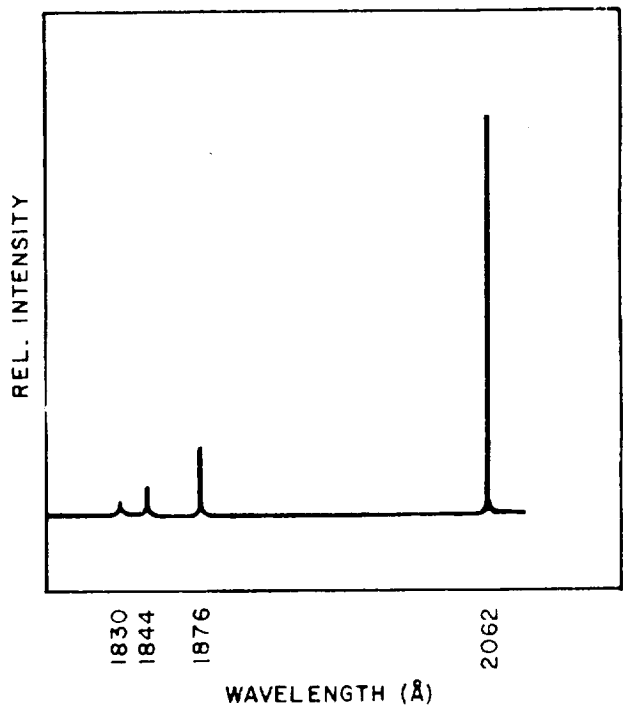

Figure 16. Spectral distribution of intensity from the iodine vapor lamp in the region 1800Å–2100Å.

atmospheric oxygen. There is no line between 2062Å and 3380Å, and only weak molecular band emission was recorded. The iodine lamp was thus considered purely monochromatic for thallium iodide pair formation.

4. Ion Detector

For measuring the rate of production of ions and the output yield of the uv lamps, a simple ion chamber was constructed (figure 17). The cylindrical electrode was made of expanded tantalum mesh and the inner electrode was a 40/1000" tantalum wire. The envelope was made of Pyrex glass with a LiF window for the iodine experiment and a quartz window for the thallium iodide experiment. The molecular vapor pressure was controlled by adjusting the temperature of the material in a side-arm kept cooler than the ion chamber itself. If I is the intensity of the lamp (measured in photons per second) in the spectral region where the selected photoionization process takes place, L the length of the ion chamber, σ the photoionization cross section, N the number of molecules per cm^3, T the transmittance of the window material, the number of ion pairs produced per second is

$$\Gamma = d\,n/d\,t = I\,T\,[1 - \exp(-\sigma N L)]$$

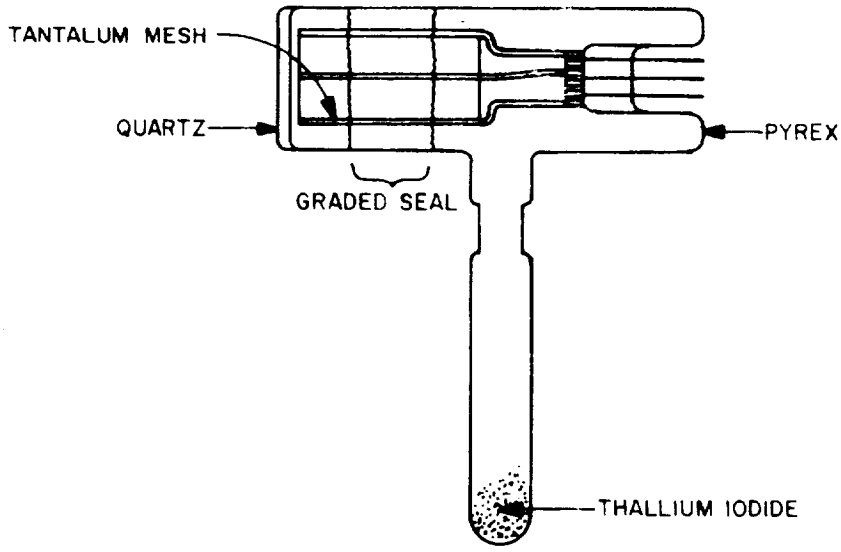

Figure 17. Design of photoionization chamber using photo production of ion pairs in Tl to calibrate the iodine lamp.

Now in general the equation governing the ion density is

$$d\,n/d\,t = \Gamma + D\,\nabla^2\,n - K\,\nabla\cdot(n\,E) - \alpha\,n^2$$

where D is the diffusion coefficient, K, the ionic motility, E the applied electric fields, α the recombination coefficient and Γ the rate of production. If V is the DC potential applied between the electrodes, the electric field with cylindrical geometry is given by

$$E = \frac{V}{r\,\log\,(b/a)}.$$

From the Einstein relation KD = e/kT, one can deduce the relative influence of the electric field and diffusion, which is given by the ratio

$$\frac{K\,V}{D\,\log\,b/a}.$$

The ratio is approximately unity for V = 10 volts. The ion current vs voltage curve rapidly saturates at a few volts and then stays constant, (figure 18).

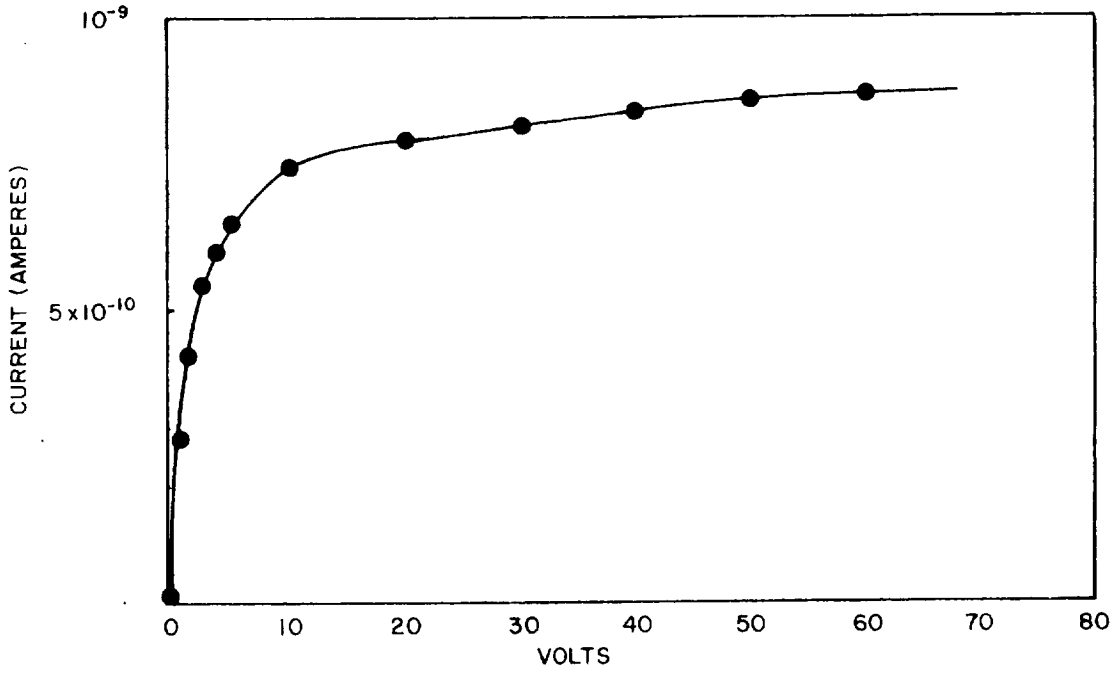

Figure 18. Iodine photo-detector current vs voltage for krypton lamp operating at 20 watts. Iodine vapor pressure was approximately 8×10^{-4} torr.

When no DC potential is applied, the equilibrium density is the solution of the equation:

$$- D \nabla^2 n + \alpha n^2 = \Gamma$$

The analysis of Gray and Kerr, for an infinite cylinder, shows that the quantity

$$\beta = \frac{\alpha n_0 R^2}{5.7 D}$$

measures the extent to which the density is initially recombination controlled ($\beta \gg 1$) or diffusion controlled ($\beta \ll 1$).

The density can be obtained by measuring the dielectric constant of the plasma

$$\epsilon = \epsilon_0 \left(1 - \frac{\omega_p^2}{\omega (\omega + i \nu_c)}\right)$$

where ν_c is the momentum transfer collision frequency, and ω_p the plasma frequency, related to the ion density by the relationship

$$\omega_p^2 = n\, e^2 \left(\frac{m_1 + m_2}{m_1\, m_2} \right)$$

where m_1 and m_2 are the ionic masses. The magnitude and phase of the ion plasma dielectric constant was measured with a lock-in amplifier. The vapor pressure and the lamp output were reduced to have a plasma frequency within the range of the lock-in amplifier (maximum detection frequency 150 kHz). The experimental curves are shown in figure 19. From the deduced plasma frequency, a value for the equilibrium ion density was obtained. The photon yield of the lamps increased nearly linearly with the power (figure 20). For given conditions of the lamp and the voltage between the electrodes of the detector, the collected current was measured as a function of the pressure in the detector (figure 21).

In the case of the krypton lamp, with iodine vapor pressures lower than 10^{-3} torr, the measured ion current was larger than expected from Lambert's law. This is attributable to the photoelectrons emitted by the tantalum mesh. From the values

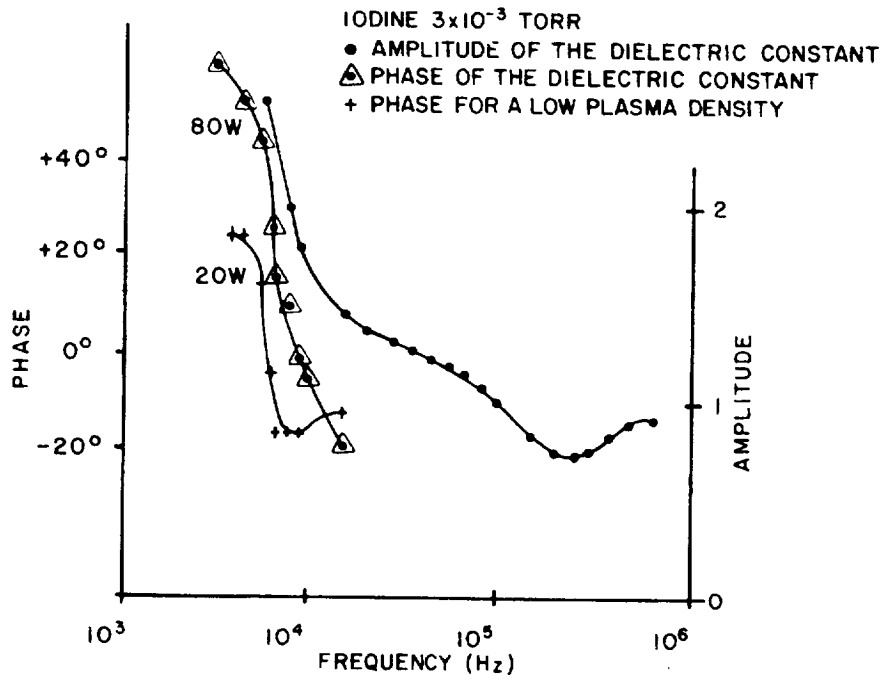

Figure 19. Results of dispersion measurements using the iodine photodetector. Ion pairs produced by irradiation with the krypton lamp.

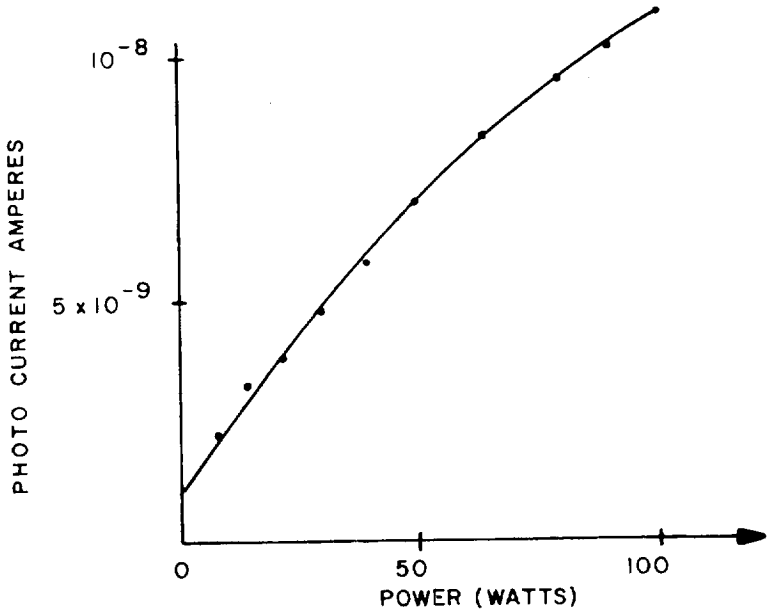

Figure 20. Photo current in iodine detector versus the power input to the krypton lamp. Iodine vapor pressure $\approx 10^{-3}$ torr.

of the photoionization cross section for pair formation in iodine, as published by Samson, and using the published vapor pressure data for I_2 the deduced maximum photon yield of the krypton lamp was 4×10^{13} photons/sec/steradian, in the spectral range of 1320Å - 1410Å. This value proved to be insufficient to observe any confined iodine plasma in a quadrupole trap.

In the case of the iodine lamp the maximum measured output was 2×10^{15} photons/sec/steradian. The rate of production of ion pairs was measured with the ion detector filled with TlI. For this purpose, the detector window was made of quartz. The rate of production could be measured only in the range of 10^{-4} - 10^{-2} torr and was found to vary linearly with the pressure, according to the Lambert Law in the region of low absorption.

EXPERIMENTAL PROCEDURE AND RESULTS

Preliminary observations were made by producing the ions by electron bombardment. A tungsten filament (.005") was heated by a DC current of about 2A. An accelerating voltage was applied between the filament and the lower cap electrode. With iodine vapor, both positive and negative ions were observed. The negative ions were produced in greater number when the accelerating voltage was increased over 50V. A possible explanation is that the electrons, produced secondary electrons from the tantalum mesh with very low energy near the metal surface and could then yield negative ions, [15] according to

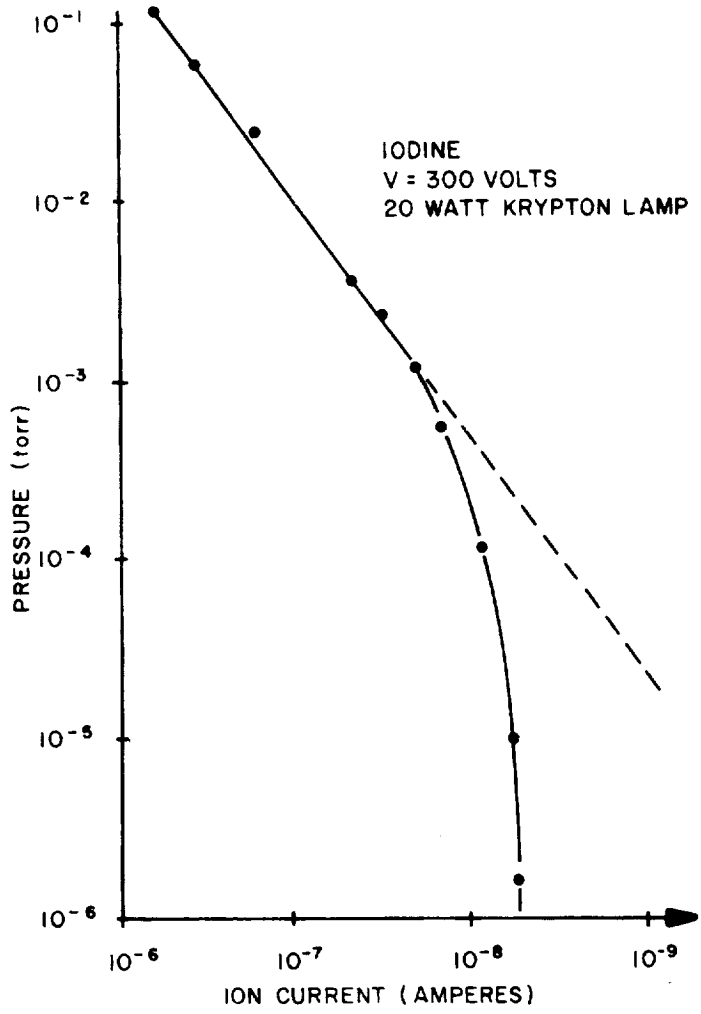

Figure 21. Photo current in iodine detector versus iodine vapor pressure for fixed input power to krypton lamp (20 watts).

$$I_2 + e \rightarrow I^- + I$$

With thallium iodide, positive thallium ions and negative iodine ions were observed, as well as positive iodine ions. An attempt to observe negative thallium ions [16] was unsuccessful.

When the trap was illuminated with the uv lamps, a photoelectron current could be measured by connecting the cylinder and the lower cap and applying a DC voltage between these electrodes and the upper cap. With the krypton lamp irradiating iodine vapor in the trap, positive ions produced by photoelectrons were readily observed, although no negative ions due to pair formation were

observed. The longer wavelength iodine lamp, on the other hand, produced only 10^{-9} A of photoelectron current, due to the work function of tantalum. With thallium iodide, the trap was operated with applied voltages corresponding to $a_z = -0.028$ and $q_z = 0.365$ for the Tl^+ ions, yielding a detection frequency of 23 kHz. When the intensity of the iodine uv lamp was changed, a shift appeared in the DC potential for which the ion resonance was observed. This shift is compared in figure 22 with the values predicted by the model of two ion clouds coupled by the electrostatic interaction. The vapor pressure of thallium iodide, for optimum operation, was 4×10^{-7} torr, and helium was added at a pressure of 10^{-4} torr. The decay-time measurements indicated that for these pressures, recombination was the most important ion-loss mechanism. The rate equation was then

$$dn/dt = I k_1 k_2 T \sigma N_0 z_0 - \alpha n^2$$

where n is the ion density, I the light output, k_1 a geometrical factor corresponding to the quartz optics and trap acceptance angle, T the mesh transparency (62%),

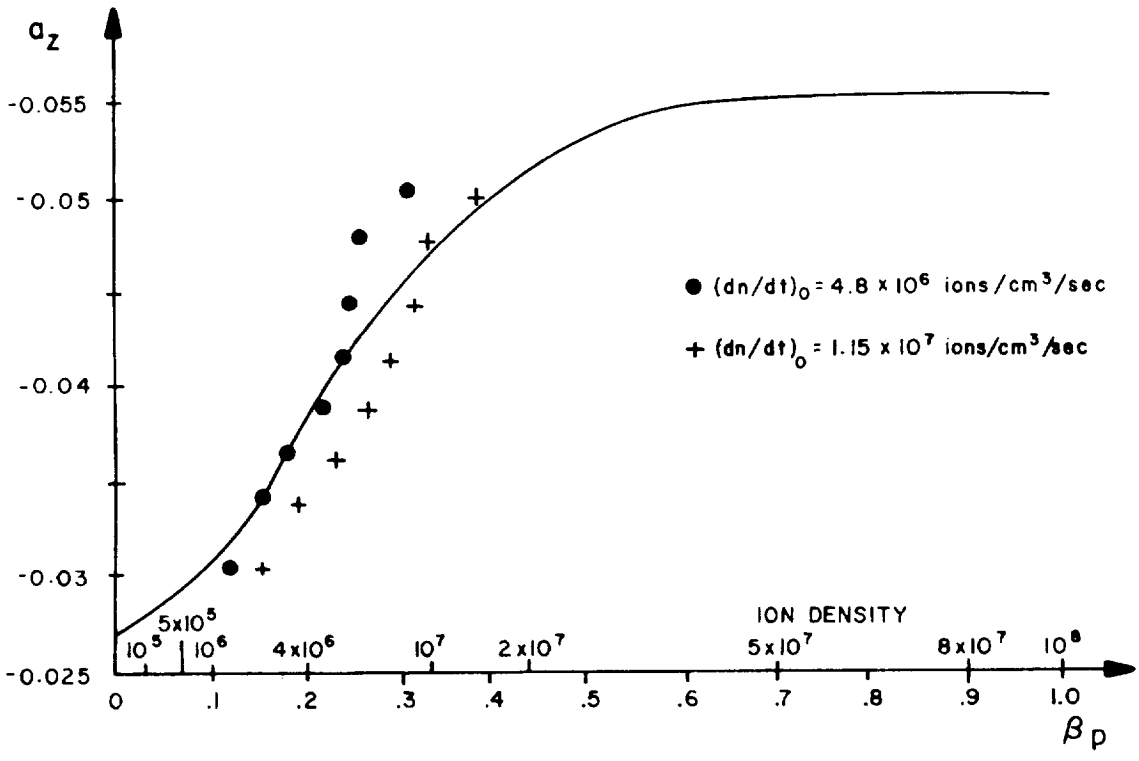

Figure 22. Plot of theoretical curve of a_z for Tl^+ ion versus the ion density showing also some experimental points for different assumed absolute ion production rates.

σ the photoionization cross section for pair formation, N_0 the molecular density, α the recombination coefficient, and k_2 is the ratio of the number of ions created in the trap to the number of ions actually confined, averaged over the initial phase of the RF field. For $\beta_z = 0.2$, $k_2 = 0.66$. The steady state value of the density is thus proportional to the square root of the light intensity. A best fit of the experimental values with the theory was obtained by taking $\alpha = 6 \times 10^{-8}$ $cm^{-3}/sec.$, and a rate of production of 4.8×10^6 ions/cm^{-3} sec. at 4×10^{-7} torr of of the thallium iodide.

The value computed from the ion detector measurements is 1.1 10^7 ion cm^{-3}/ sec at the same pressure of 4×10^{-7} torr.

By interrupting the uv radiation with a shutter and varying the time delay between the end of the formation period of the ions and their detection, the time dependence of the ion population decay was measured. For a sufficiently large AC voltage applied to the trap, (i.e., large q_z value), only thallium ions may be confined. Without helium added, the collisions of the ions with the molecular background lead to a rather short (in the context of the present work) life-time of one second. The ratio between the masses of helium and thallium being approximately 50, the helium pressure has to be two orders of magnitude higher than the molecular pressure, to have a cooling effect. This is shown in figure 23. For 10^{-4} torr of helium, the ion life time was increased to 8 seconds.

When both iodine and thallium ions were trapped, it was verified that the time dependence of the two ion populations was the same. For a high helium pressure, the experimental time dependence (figure 24), can be fitted with a decay

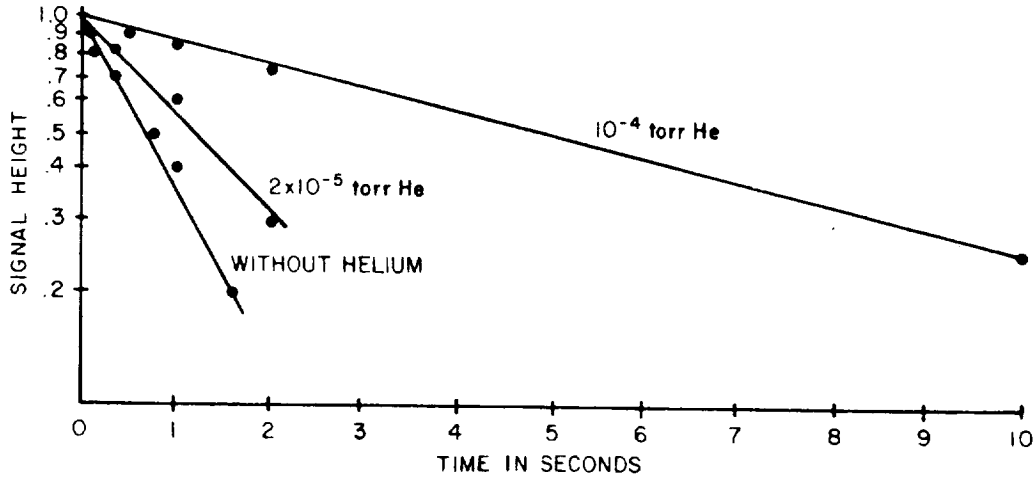

Figure 23. Signal height of (Tl^+) confined alone as a function of delay after closing the light shutter.

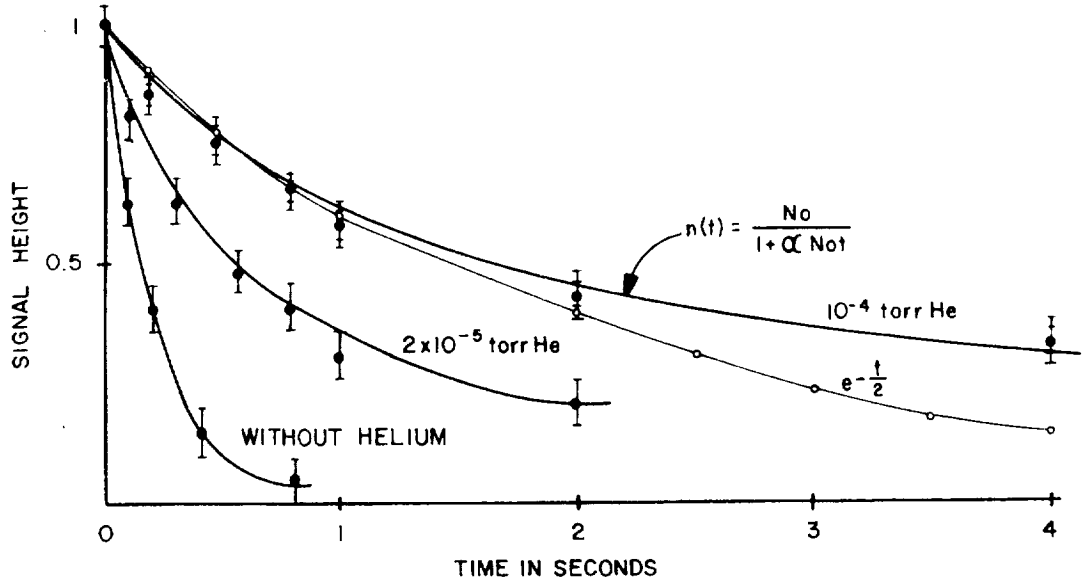

Figure 24. Signal height of Tl^+ confined simultaneously with I^- as a function of the delay after closing the light shutter.

having the form

$$n(t) = \frac{n(0)}{1 + \alpha\, n(0)\, t}$$

Assuming the value of n(o) obtained by measuring the DC shift of the ion resonance, the best fit was obtained for $\alpha = 6 \times 10^{-8}$ cm^3/sec. The experimental value obtained by Fisk[17] was $\alpha = 4 \times 10^{-8}$ cm^3/sec. at thermal energies. The uncertainty in the trapped ion temperature prevents an accurate comparison of the values of α. However there is agreement within the broad errors of the experiment and assumptions of the analysis.

FUTURE WORK

The resonance frequency shift measurement should be extended to the iodine negative ion and it should be verified that the ion resonance frequency shift, being a measure of the ion density, changes as a function of time, when a lifetime measurement is performed.

For given conditions of light intensity and trapping voltages, it would be interesting to excite and measure the resonance frequency of one species (e.g. iodine)

while monitoring the amplitude and shift of the resonance signal of the other species (thallium). This double resonance experiment could give information on the densities of either species as affected by the presence of the other. In order to demonstrate the improvement due to the space-charge neutralization, the potential well (given by the secular motion frequency ω_z) should be reduced to a value corresponding to a small theoretical value for the space charge limited density (e.g. 5×10^5 ions/cm^3). It could be fruitful to investigate the confinement of a plasma with an RF trapping frequency lower than the plasma frequency ω_p. For $\omega_p < \Omega$ (low density), the ionic medium is transparent. For $\omega_p > \Omega$ the alternating voltage will only penetrate the plasma over a length equal to the skin depth. The frequency of motions of the ions inside this volume could be strongly affected.

The ionic density could also be monitored, as a function of time, by observing the decay of the fluorescence light due to recombination.

REFERENCES

1. F. G. Major, "Microwave Resonance of Field-Confined Mercury Ions for Atomic Frequency Standards," Goddard Space Flight Center, Greenbelt, Md. Document X-521-69-167 (May, 1969).

2. P. Davidovits, J. Hirschfield, Applied Physics Letters 15 290 (1969).

3. H. Doucet, Physics Letters 33A 283 (1970).

4. G. Herzberg, "Spectra of Diatomic Molecules," Van Nostrand (1950).

5. J. Berkowitz, W. Chupka, J. Chem. Phys. 45 1287 (1966).

6. J. Myer, A. Samson, J. Chem. Phys. 52 716 (1970).

7. V. Dibeler, J. Walker, J. Opt. Soc. Am. 57 1007 (1967).

8. D. Bates, T. Boyd, Proc, Phys. Soc. A69 910 (1956)

9. E. Fischer, Z. Physik 156 1 (1967)

10. W. Paul, O. Osberghaus, E. Fischer, Forschungsber. Wirtsch. Verkehrsministeriums Nordrhein-Westfalen 415 (1958).

11. H. Schussler, N. Forston, H. Dehmelt, Phys. Rev. 187 186 (1969).

12. D. Rose, M. Clark, "Plasmas and Controlled Fusion," J. Wiley (1961).

13. F. G. Major, H. G. Dehmelt, Phys. Rev. 170 91 (1968).

14. J. Samson, "Techniques of Vacuum Ultraviolet Spectroscopy," J. Wiley (1967).

15. F. Truby, Phys. Rev. 188 508 (1969).

16. V. Khovostenko, A. Sultanov, JETP 19 1086 (1964).

17. G. Fisk, J. Chem. Phys. 47 2649 (1967).